

Modeling of Tunneling Current of Electron in Bilayer Armchair Graphene Nanoribbons P-N Junction Diode Using Transfer Matrix Method

Intan Anjaningsih¹, M. Fulki Fadhillah¹, Lilik Hasanah¹ and Endi Suhendi^{1*}

¹Program Studi Fisika, Universitas Pendidikan Indonesia, Bandung, Indonesia.

Received 28 June 2019, Revised 2 September 2019, Accepted 22 October 2019

ABSTRACT

The tunneling current in the P-N junction diode Bilayer Armchair Graphene Nanoribbons (BAGNR) was calculated. The tunneling current was obtained by solving the Schrödinger equation to find out the electron transmittance through a potential barrier by using the Transfer Matrix Method (TMM). The tunneling current was calculated for various variables such as bias voltage, BAGNR width, electric field, and temperature. It is found that the tunneling current increases with the increasing bias voltage. Furthermore, the tunneling current of electron increases with the increasing BAGNR width or the applied electric field, otherwise it decreases with the increasing temperature. The tunneling current of P-N junction diode BAGNR generated approximately 4.8 μA with 1 MV/cm electric field and a bias voltage of 100 mV. Then, the calculation of tunneling current of BAGNR was also compared with Monolayer Armchair Graphene Nanoribbons (MAGNR). By using BAGNR, the tunneling current produced is three times greater than using MAGNR. In addition, the tunneling current using TMM is then compared with the Wentzel-Kramers-Brillouin (WKB) method and shows that these two methods produce the same value at a low voltage below 30 mV, while at high voltages, MMT always has a higher value.

Keyword: Tunneling Current, P-N Junction Diode, BAGNR, TMM.

1. INTRODUCTION

Graphene was first synthesized in 2004 by scientists namely Andre Geim and Kostya Novoselov in University of Manchester [1]. Graphene or monolayer graphite is a two-dimensional layer with a thickness of one single atom in a tight bond of carbon atoms forming a hexagonal crystal structure [1]. Graphene has a high electrical conductivity at room temperature with mobility reaching $15,000 \text{ cm}^2\text{V}^{-1}\text{s}^{-1}$ under ambient temperature and can be increased to reach $\sim 100,000 \text{ cm}^2\text{V}^{-1}\text{s}^{-1}$ at 300 K [1,2]. The carrier mobility in graphene is one hundred times greater than carrier mobility in silicon which has carrier mobility around $1400 \text{ cm}^2/\text{Vs}$ [3]. This high charge carrier mobility value is required for high-speed electronic devices. With its extraordinary properties, graphene has the potential to be applied to various electronic devices today and has promising potential for the future.

The graphene bandgap can be changed by reducing its size to a nanoscale. Graphene at this size is called Graphene Nanoribbon (GNR) [4]. In addition, graphene can be changed by making two layers of graphene or commonly called bilayer graphene to improve its properties.

*Corresponding Author: endis@upi.edu

Bilayer graphene has better properties than monolayer graphene, bilayer graphene has unique features such as anomalous integer quantum Hall effect [5] and the ability to control the size of the energy gap (E_g) by adjusting carrier concentration [6] as well as by external electric field [7]. With these properties, bilayer graphene can be applied more widely in various applications. The electronic properties are depending on the ribbon width as well as the atomic configuration of the edges. The Armchair Graphene Nanoribbons (AGNR) edge structure can be either metallic or semiconductor depend on the width, while the Zigzag Graphene Nanoribbons (ZGNR) structure is only metallic properties independent with the width. Because the type of AGNR which can be as a semiconductor and bilayer graphene is superior compared to monolayer graphene, Bilayer Armchair Graphene Nanoribbons (BAGNR) can be developed and used on various electronic devices and can be a basic material for P-N junction diode [8,9]. Previously, some researchers have reported that Monolayer Armchair Graphene Nanoribbon (MAGNR) can be applied to P-N junction diodes and other more complex electronic devices such as in fabrication of ultrafast transistors, TFET, etc. [10–14] and show better performance than devices with conventional semiconductors, but still has limited abilities because it has a wide energy gap. Therefore, in this study, BAGNR was used to improve the abilities in a P-N junction diode

P-N junction diodes are formed from P-type and N-type semiconductors. In order to produce P-type semiconductors, BAGNR can be doped with Boron, whereas to produce N-type semiconductors, BAGNR can be doped with Nitrogen [15]. Boron and Nitrogen-doped bilayer graphene were synthesized by arc discharge using boron-packed graphite electrodes and in the presence of ammonia, respectively [16].

To compute the tunneling current in GNR-based devices, several methods have been carried out such as Airy Function Approximation (AFA), Wentzel-Kramers-Brillouin (WKB) and Transfer Matrix Method (TMM). Data from several studies suggest that TMM is the best method for calculating the tunneling current [10,17–19].

In this study, we modeled the tunneling current of electron on the P-N BAGNR junction diode by using the Schrodinger equation wave function to obtain the transmittance of electrons through a potential barrier using the transfer matrix method, which is a numerical approach better than WKB. Tunneling current of the electrons was generated and analyzed by computing the effect of the bias voltage, electric field on the potential barrier, width of the BAGNR and the temperature on the P-N junction diode. The BAGNR width depends on the N index value, which is the number of atomic rows on the wide side of BAGNR. The results of the tunneling currents of electron on the P-N BAGNR junction diode with TMM are then compared with MAGNR and by the WKB method. Then, to calculate and visualize the potential barrier, electron transmittance and the tunneling current of diode we use MATLAB which is a graphical user interface.

2. THEORETICAL MODELS

The electronic dispersion relation in BAGNR at low energy in the parabolic region is given by [20]:

$$E(\mathbf{k}) = \pm \hbar^2 k^2 / 2m^* \quad (1)$$

Where m^* is the effective mass of charge carrier that is $m^* = \gamma_1 / 2v_F^2$ and $k = \pi n / 3w$ is momentum where w is the width of BAGNR, which is influenced by N index. Then, the value of n is $n = \pm 1, \pm 2, \pm 3, \dots$ [21].

In the case of isotropic graphene, it is assumed that the energy gap depends only on the Fermi velocity and bandwidth [21], then the BAGNR energy band gap at the low energy state becomes:

$$E_g = \frac{\hbar^2 \pi^2 v_F^2}{9w^2 \gamma_1} \quad (2)$$

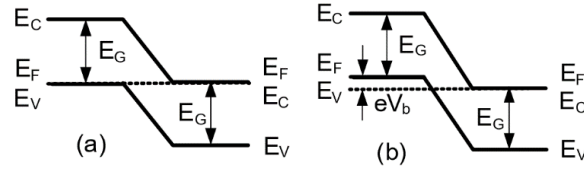


Figure 1. (a) Electricity Potential Profile of P-N junction in thermal equilibrium conditions, (b) profile of P-N electrical potential when reverse biased applied [22].

Figure 1. (a) is an energy band diagram of P-N junction in a thermal equilibrium state based on the P-N junction energy band structure, with no bias-voltage and without flowing current. In this condition, it is assumed that the P side and N side dopant causes the Fermi energy level (E_F) of the BAGNR semiconductor to be in the valence band in P regions and in the conduction band in N regions [22]. Then, in figure 1. (b) the energy band diagram of the P-N junction diode when given a reverse bias (V_R). The reverse bias voltage causes the valence band in part P to be higher than the conduction band in part N. This bias voltage causes electrons from the valence band in part P to tunneling the depletion area to the conduction band in part N known as the Zener tunneling [23]. Then, we assumed that the doping concentrations in the N-type and P-type BAGNR are the same, so the barrier potential refers to ref. [10]. Therefore, the width of the depletion region in the P regions and N regions are equal, that is $d = E_g/eF$, where E_g is the band gap energy, e is the electronic charge, F is the electric field in the depletion region, and d is the depletion region thickness [22]. Thus, the potential profile refers to ref. [10].

To calculate the electron transmittance, we employ the transfer matrix method (TMM). In this method, the potential profile is divided into n segments and the wave function was obtained by divide the profile potential into four regions. Additionally, the electron transmittance in the BAGNR P-N junction diode was compered by WKB. In the WKB methods the profile potential is not divided into n segment but used a formula there are refers to ref. [22]. Then, the analytical expression of the electrons transmittance is derived by using an exponential solution of the Schrödinger equation and by applying the boundary condition of the potential profile in ref. [10]. Whereas, the tunneling current in the P-N BAGNR junction is expressed by equation (3) [22]:

$$I = \frac{2g_v e}{h} \int_0^{eV} [f_v(E) - f_c(E)] T(E) dE \quad (3)$$

With

$$f_v(E) = (1 + \exp[(E - eV_b)/(k_B T)])^{-1} \quad (4)$$

And

$$f_c(E) = (1 + \exp[E/(k_B T)])^{-1} \quad (5)$$

which is the Fermi-Dirac distribution function for electrons in the valence band and conduction band, k_B is the Boltzmann constant, h is the Planck constant, g_v is the degeneration of BAGNR ($g_v = 1$) and $T(E)$ is transmittance. Then, all of the steps are calculated by MATLAB.

3. RESULTS AND DISCUSSION

Figure 2 shows the results of the calculation of electron transmittance. The value of the energy gap in BAGNR is 0.11 eV, greater than the electron energy in this calculation. For the electron energy value of 0.001 eV, the transmittance obtained is more than zero, which is about 0.5. This means that there are electrons that succeed tunneling through the potential barrier. The greater the energy value of the electrons that come, the more electrons that can tunneling the potential barrier so that the transmittance is higher, which is close to 1, this is accordingly with the research that has been done before [17,24]. In these conditions, most electrons have enough energy to tunnel a potential barrier wall so that the electrons transmission the potential barrier walls become numerous [11].

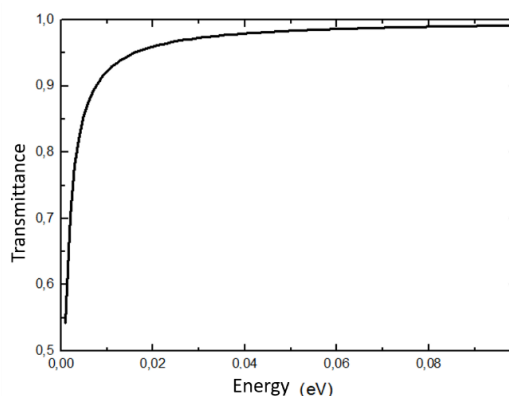


Figure 2. Electron transmittance of P-N BAGNR junction diodes.

Figure 3 shows the results of the calculation of the tunneling current as a function of applied bias voltage with different N index values. This graph is plotted using equation (3), where the electron transmittance is affected by the energy gap. The energy gap is influenced by the N index which affects the width of the band. In this picture, there is a significant increase in the current along with the increase in the value of $N = 22$ to $N = 28$, but for $N = 28, 34$ and 40 the transition is not significant even though the tunneling current still rises. If the value of n is greater, the number of atoms that comprise the P-N junction diode is increasing, so the number of charge carrier particles will increase. When the number of particles carrying charge (in this case is electrons) increases, the value of the current produced will be higher. Previous research shows that the electronic structure of the AGNR is greatly affected by the width of the ribbon, which is influenced by the index value of N [25]. A graphene nanoribbon system will be a conductor when $N = 3p + 2$ and is a semiconductor or metallic for $N = 3p$ and $N = 3p + 1$ with p are integer (1,2,3,...) [8,25]. In this study, we use $N = 3p + 1$ (with $p = 4; 5; 6; 7$) for semiconductors because it is used for diode devices.

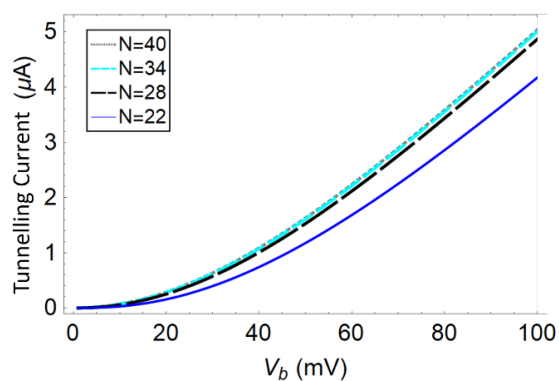


Figure 3. The tunneling current as a function of the bias voltage with various N .

The results are in accordance with several studies that have been done before, which shows that the BAGNR energy gap decreased with the increase in the width of the ribbon [25–31]. In a study conducted by Jena, et al. (2008) current density increases with increasing GNR width and reaches a maximum when the width of the AGNR reaches a certain value, namely w_0 [22]. When the width exceeds this w_0 , the tunneling current will saturate because one of the conditions for the tunneling process to occur in the P-N junction diode is that the depletion width must be very thin [23]. In this study, we varied the width of the BAGNR from ~ 2.5 nm ($N = 22$) to $w = \sim 5$ nm ($N = 40$) and show that the tunneling current has a significant increases for $N = 22$ ($w = 2.58$ nm) to $N = 28$ ($w = 3.32$) because the width is predicted to be below the value of w_0 . While, for $N = 28, 34$ and 40 the changes of tunneling current is very minimal because it is predicted to have reached saturation and the width exceeds the w_0 .

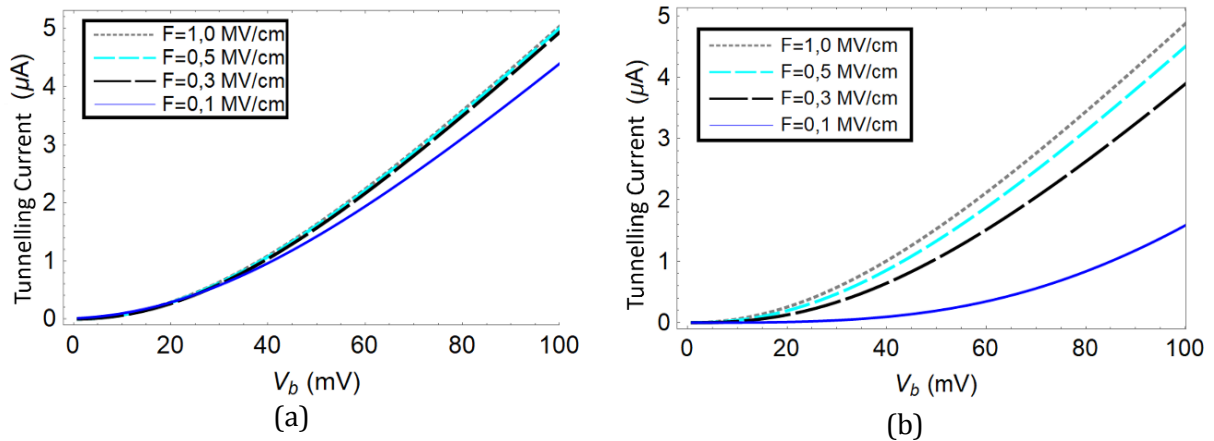


Figure 4. The tunneling current as a function of the bias voltage with an electric field variation $F = 0,1$ MV/cm; $0,3$ MV/cm; $0,5$ MV/cm; and 1 MV/cm for (a) $N = 40$ and (b) $N = 28$.

The results of the calculation in Figure 4 (a) show the tunneling current of the bias voltage with $N = 40$ and Figure 4 (b) for $N = 28$ at room temperature (300 K) based on equation (3) where the variation of electric field influenced the potential barrier, so the transmittance affected [10]. Both of these graphs show that the tunneling current is higher when the electric field is greater, which means that the electron which tunneled the potential barrier walls is increasing. With the increasing electric field, electrons traversing the depletion layer obtain higher and higher kinetic energy, thereby the density of tunneling current is increased [24]. Some atoms will have enough energy to raise an electron from the valence band to the conduction band which occurs because of the release of covalent bonds, thereby creating an electron-hole pair. This phenomenon is called the impact of ionization [23]. But we find the difference in the result of tunneling current for $N = 40$ and $N = 28$ with the same electric field variation. This difference can occur because for a larger BAGNR width (greater N) the tunneling current will be easier to reach up to its maximum point until it reaches saturation there is when the width reach w_0 because of an increase in the carrier of charge will increase the number of electrons that get additional energy when the electric field is applied in the depletion. While for smaller BAGNR widths (smaller N) the maximum tunneling current is not easily achieved.

The tunneling current phenomenon in P-N junction can occur if the electric field in the junction is large enough. On P-N junction diodes made from ordinary semiconductors such as Silicon (Si) with an energy band gap of 1.14 eV, the required electric field reaches 15 MV/cm to produce a tunneling current of about ~ 1.3 μ A with a device width of 3.32 nm. While in BAGNR with the same width, the electric field needed to produce the tunneling current is only about 0.1 MV/cm which is much smaller than the P-N junction diode with silicon material. For example, in order to produce an electric field around 1 MV/cm in ordinary semiconductors requires a large doping

concentration of about $> 5 \times 10^{17} \text{ cm}^{-3}$ in the P region and the N region [23]. Whereas for the BAGNR, the required doping concentration will be much smaller [15].

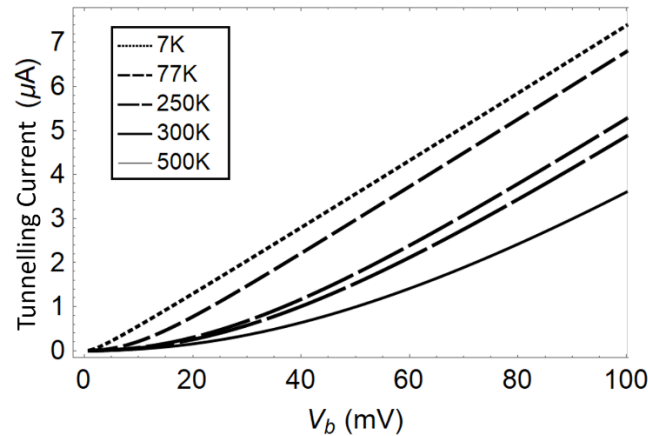


Figure 5. The tunneling current as a function of bias voltage with temperature $T = 7 \text{ K}, 77 \text{ K}, 250 \text{ K}, 300 \text{ K}$ and 500 K .

Figure 5 shows the plot of the calculation of tunneling current as a function of bias voltage with the temperature varied. In the picture, the tunneling current is inversely proportional to the temperature. This means that an increase in temperature will reduce the tunneling current [12]. When the temperature raises, a thermal resistivity raises too so the tunneling current decreases. This thermal resistivity occurs due to electron collisions which increase as the temperature increases. The results of this calculation are in accordance with the research that has been done before on the GNR-based P-N diode [10,22].

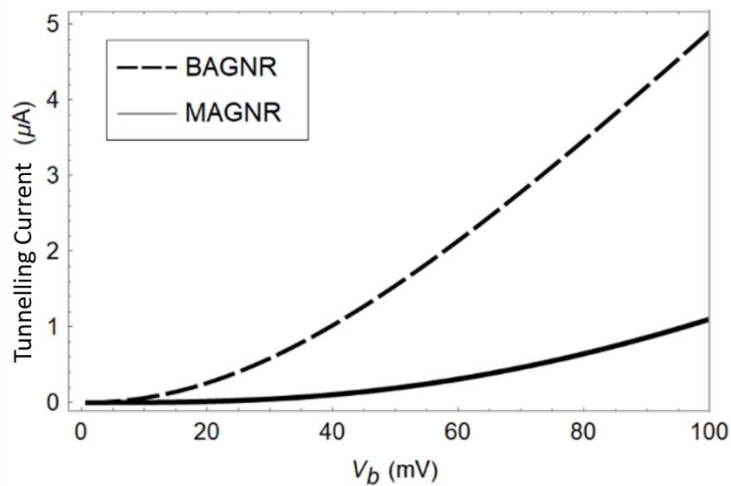


Figure 6. The comparison plot of the tunneling current as a function of the bias voltage for MAGNR and BAGNR.

Figure 6 shows a plot of the comparison of the results of the tunneling current calculation as a function of bias voltage using MAGNR and BAGNR. In these calculations, we used the width parameter AGNR $w = 3.32 \text{ nm}$ ($N = 28$), the electric field $F = 1 \text{ MV/cm}$ and the temperature $T = 300 \text{ K}$, interlayer coupling $\gamma_0 = 2.6 \text{ eV}$ for both MAGNR and BAGNR and for BAGNR interlayer couplings are used $\gamma_1 = 0.3 \text{ eV}$. Based on the results of calculations obtained an energy gap for MAGNR of 0.35 eV with a depletion width of 3.49 nm this value is obtained based on the disperse relations [17]. While for BAGNR the energy gap obtained from the calculation is equal to 0.102 eV with a depletion width of 1.02 nm . The BAGNR energy gap value is much smaller than the MAGNR and the BAGNR depletion width is much thinner than MAGNR, so the electrons

will be much easier to penetrate through the potential barrier walls of the BAGNR than MAGNR [32].

The energy band structure of the graphene bilayer is influenced by γ_0 , which is the hopping parameter in the same plane $A_j \leftrightarrow B_j$, γ_1 is hopping parameter $A_1 \leftrightarrow A_2$, γ_3 is hopping parameter $B_1 \leftrightarrow B_2$ and γ_4 is hopping parameter $A_1 \leftrightarrow B_2$ or $A_2 \leftrightarrow B_1$. In this study only the influence of interlayer coupling γ_0 and γ_1 was reviewed, because these two parameters directly influence the energy gap of BAGNR. Whereas in MAGNR, the hopping parameter that affects the energy band gap is only γ_0 because MAGNR is only composed of a layer of carbon atoms. As a result, the tunneling current on BAGNR increases much more than MAGNR because BAGNR is not only affected by the interlayer coupling γ_0 , but is also influenced by the interlayer coupling parameter γ_1 which is proportional to the effective mass of the load carrier thus decreasing the energy gap in BAGNR [20,33]. Meanwhile, the hopping parameter γ_0 affects the Fermi velocity n BAGNR and MAGNR. The relation γ_0 with Fermi velocity is shown in equation $v_F = \frac{3\gamma_0 a}{2\hbar}$ [34], where $a = 1,42\text{\AA}$ is the distance between carbon atoms.

This Fermi velocity value affects the effective mass of charge carriers on BAGNR and MAGNR. The charge carrier in a conductor crystal or semiconductor has a certain effective mass depending on the crystal structure. For graphene bilayer, the effective mass of the charge carrier with Fermi velocity is connected by the equation $m^* = \gamma_1/2v_F^2$ [35], while the effective mass MAGNR of Fermi velocity is related to the equation $m^* = E_g/2v_F$.

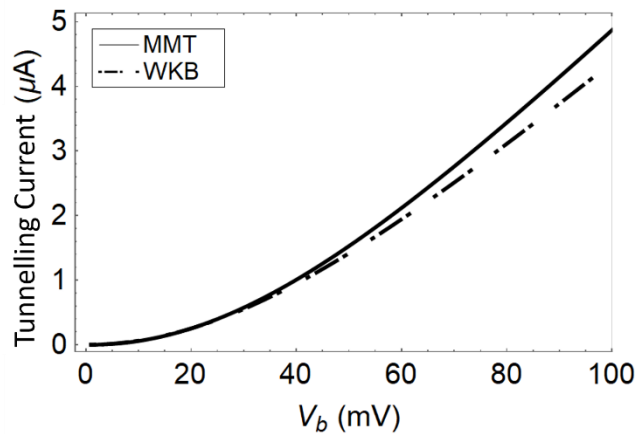


Figure 7. Tunneling current plot of the bias voltage with a different method, $F = 0.1 \text{ MV/cm}$.

Figure 7 shows a tunneling current which is calculated as a function of the applied bias voltage. In calculations, the width of BAGNR is 3.32 nm ($N = 28$), the electric field in the depletion area is 1 MV/cm, and the temperature used is 300 K. It was found that the tunneling current was obtained by the MMT and WKB methods increases when the bias voltage increases. All calculated tunneling currents are equal at a low bias voltage of less than 30 mV. A further increase in the bias voltage makes the tunneling current calculated by the WKB method always lower than that obtained by the MMT method [10,36].

4. CONCLUSION

The tunneling current on the P-N BAGNR junction diode is influenced by BAGNR width, electric field, and temperature. The increases in the width of the BAGNR, the greater the electric current produced. Similarly, when the electric field applied is getting higher, the resulting tunneling current is higher too. In this calculation, the tunneling current is obtained at a voltage of 100 mV with $N = 28$ with an electric field variation of around 1.3-5.0 μA . Meanwhile, for $N = 40$ the

tunneling current obtained is around 4.0-5.0 μA . Meanwhile, the increase in temperature will reduce tunneling current. BAGNR has better properties than MAGNR if it is applied to the P-N junction diode. Calculation of tunneling current using MMT is more accurate than the WKB method and the MMT has also been used as the calculation standard.

ACKNOWLEDGMENT

This work was financially supported by “Hibah Penelitian Berbasis Kompetensi” Research Grants in the fiscal year 2018, KEMENRISTEKDIKTI Republic of Indonesia.

REFERENCES

- [1] A. K. Geim and K. S. Novoselov, “The rise of graphene,” *Nat. Mater.* **6**, Maret (2007) 183–191.
- [2] B. Alemour, M. H. Yaacob, H. N. Lim & M. R. Hassan, “Review of electrical properties of graphene conductive composites,” *Int. J. Nanoelectron. Mater.* **11**, 4 (2018) 371–398.
- [3] C. Jacoboni, C. Canali, G. Otiaviani & A. A. Quaranta, “A Review of Some Charge Transport Properties of Silicon,” *Solid State Electron.* **20** (1977) 77–89.
- [4] A. H. Castro Neto, F. Guinea, N. M. R. Peres & K. S. Novoselov, “The electronic properties of graphene,” *Am. Phys. Soc.* **54**, 1 (2009) 109–162.
- [5] K. S. Novoselov, E. McCann, S. V. Morozov, V. I. Fal'ko, M. I. Katsnelson, U. Zeitler, D. Jiang, F. Schedin & A. K. Geim, “Unconventional quantum Hall effect and Berry’s phase of 2π in bilayer graphene,” *Nat. Phys.* **2**, 3 (2006) 177–180.
- [6] T. Ohta, A. Bostwick, T. Seyller, K. Horn & E. Rotenberg, “Controlling the electronic structure of bilayer graphene,” *Science* (80-.). **313**, 5789 (2006) 951–954.
- [7] E. V. Castro, N. M. R. Peres & J. M. B. L. Dos Santos, “Gaped graphene bilayer: Disorder and magnetic field effects,” *Phys. Status Solidi Basic Res.* **244**, 7 (2007) 2311–2316.
- [8] L. Brey & H. A. Fertig, “Electronic states of graphene nanoribbons studied with the Dirac equation,” *Am. Phys. Soc.* **73**, 235411 (2006) 2–6.
- [9] K. Nakada, M. Fujita, G. Dresselhaus & M. S. Dresselhaus, “Edge state in graphene ribbons: Nanometer size effect and edge shape dependence,” *Am. Phys. Soc.* **54**, 24 (1996) 954–961.
- [10] E. Suhendi, R. Syariati, F. A. Noor, N. Kurniasih & Khairurrijal, “Model of a tunneling current in a p-n junction based on armchair graphene nanoribbons-an Airy function approach and a transfer matrix method,” *AIP Conf. Proceeding* **91** (2014) 1–5.
- [11] E. Suhendi, R. Syariati, F. A. Noor & N. Kurniasih, “Simulation of Dirac Tunneling Current of an Armchair Graphene Nanoribbon-Based p-n Junction Using a Transfer Matrix Method,” *Adv. Mater. Res.* **974** (2014) 205–209.
- [12] E. Suhendi, R. Syariati, F. A. Noor, N. Kurniasih & Khairurrijal, “Simulation of Drain Currents of Double Gated Armchair Graphene Nanoribbon Field-Effect Transistors by Solving Dirac “Like” Equation and Using Transfer Matrix Method,” *J. Phys. Conf. Ser.* **539**, 1 (2014) 012020.
- [13] E. Suhendi, L. Hasanah, D. Rusdiana, F. A. Noor, N. Kurniasih & Khairurrijal, “Comparison of tunneling currents in graphene nanoribbon tunnel field effect transistors calculated using Dirac-like equation and Schrödinger’s equation,” *J. Semicond.* **40**, 6 (2019) 062002.
- [14] E. Suhendi, L. Hasanah, F. A. Noor & N. Kurniasih, “Modeling of Armchair Graphene Nanoribbon Tunnel Field Effect Transistors for Low Power Applications,” *J. Semicond. Technol. Sci.* **19**, 4 (2019) 336–346.
- [15] G. A. Nemnes, T. L. Mitran, A. Manolescu & D. Dragoman, “Electric field effect in boron and nitrogen doped graphene bilayers,” *Comput. Mater. Sci.* **155**, July 92018) 175–179.

- [16] L. S. Panchakarla, K. S. Subrahmanyam, S. K. Saha, A. Govindaraj, H. R. Krishnamurty, U. V. Waghmare & C. N. R. Rao, "Synthesis, structure, and properties of boron- and nitrogen-doped graphene," *Adv. Mater.* **21**, 46 (2009) 4726–4730.
- [17] A. K. Fahmi, L. Hasanah, D. Rusdiana, A. Aminudin & E. Suhendi, "Tunneling Current of Electron in Armchair Graphene Nanoribbon Bipolar Transistor Model Using Transfer Matrix Method," *IOP Conf. Ser. Mater. Sci. Eng.*, (2017).
- [18] E. Suhendi, R. Syariati, F. A. Noor & N. Kurniasih, "Modeling of Dirac Electron Tunneling Current in Bipolar Transistor Based on Armchair Graphene Nanoribbon Using a Transfer Matrix Method," *Adv. Mater. Res.* **2**, September (2015) 164–166.
- [19] F. A. Noor, R. Syariati, E. Suhendi, M. Abdullah & Khairurrijal, "Electron Tunneling Current in an n-p-n Bipolar Transistor Based on Armchair Graphene Nanoribbon by Using Airy-Wavefunction Approach," *Adv. Mater. Res.* **1112** (2015) 80–84.
- [20] S. Russo, M. F. Craciun, T. Khodkov, M. Koshino, M. Yamamoto & S. Tarucha, "Electronic transport properties of few-layer graphene materials," *arXiv Prepr. arXiv***1105.1479**, May (2011).
- [21] T. Fang, A. Konar, H. Xing & D. Jena, "Carrier statistics and quantum capacitance of graphene sheets and ribbons," *Am. Inst. Physics. Addit.* **91**, 9 (2007) 1–3.
- [22] D. Jena, T. Fang, Q. Zhang & H. Xing, "Zener tunneling in semiconducting nanotube and graphene nanoribbon p-n junctions Zener tunneling in semiconducting nanotube and graphene nanoribbon p – n junctions," *Appl. Phys. Lett.* **93**, 1 (2008)112106.
- [23] S. M. Sze & K. K. Ng, *Physics of Semiconductor Device*, Third Edit. New Jersey: John Wiley & Sons, Inc., 2007.
- [24] E. Suhendi, F. A. Noor, N. Kurniasih & Khairurrijal, "Pemodelan Efek Medan Listrik terhadap Rapat Arus Terobosan pada Sambungan p-n Armchair Graphene Nanoribbon," *Semin. Nas. Mater.*, (2013)101–104.
- [25] H. Zheng, Z. F. Wang, T. Luo, Q. W. Shi & J. Chen, "Analytical study of electronic structure in armchair graphene nanoribbons," *Phys. Rev. B* **75**, 165414 (2007) 1–6.
- [26] C. Bimo S Putro, F. A. Noor, M. Abdullah & Khairurrijal, "A Theoretical Model of Band-to-band Tunneling Current in an Armchair," *Adv. Mater. Res.* **896** (2014) 371–374.
- [27] B. Sahu, H. Min, A. H. Macdonald & S. K. Banerjee, "Energy gaps, magnetism, and electric-field effects in bilayer graphene nanoribbons," *Am. Phys. Soc.* **78** (2008) 1–8.
- [28] E. Suhendi, F. A. Noor, N. Kurniasih & Khairurrijal, "Modeling of drain current in armchair graphene nanoribbon field effect transistor using transfer matrix method," *Adv. Mater. Res.* **896** (2014) 367–370.
- [29] H. Raza & E. C. Kan, "Armchair graphene nanoribbons: Electronic structure and electric-field modulation," *Phys. Rev. B - Condens. Matter Mater. Phys.* **77**, 24 (2008) 1–5.
- [30] Y.-W. Son, M. L. Cohen & S. G. Louie, "Energy gaps in graphene nanoribbons,," *Phys. Rev. Lett.* **97**, November (2006) 216803.
- [31] L. Yang, C. H. Park, Y. W. Son, M. L. Cohen & S. G. Louie, "Quasiparticle energies and band gaps in graphene nanoribbons," *Phys. Rev. Lett.* **99**, 18 (2007) 6–9.
- [32] A. Orlof, J. Ruseckas & I. V. Zozoulenko, "Effect of zigzag and armchair edges on the electronic transport in single-layer and bilayer graphene nanoribbons with defects," *Phys. Rev. B - Condens. Matter Mater. Phys.* **88** (2013) 12.
- [33] M. Koshino, "Electronic transport in bilayer graphene," *IOP Publ.* **11** (2009).
- [34] K. Zou, "Effective mass of electrons and holes in bilayer graphene: Electron-hole asymmetry and electron- electron interaction," *Phys. Rev. B* **84**, 085408 (2011).
- [35] E. Mccann & V. I. Fal, "Landau-Level Degeneracy and Quantum Hall Effect in a Graphite Bilayer," *Am. Phys. Soc.* **086805**, March (2006) 1–4.
- [36] C. Jirauschek, "Accuracy of Transfer Matrix Approaches for Solving the Effective Mass Schrödinger Equation," *IEEE J. Quantum Electron.* **45**, 9 (2009) 1059–1067.

